

COLLISIONS OF WATER DROPS IN A GAS-VAPOR ENVIRONMENT AT HIGH TEMPERATURES AND VAPOR CONCENTRATIONS

by

Nikita SHLEGEL and Pavel STRIZHAK*

National Research Tomsk Polytechnic University, Tomsk, Russia

Original scientific paper

<https://doi.org/10.2298/TSCI191110200S>

The study of the characteristics of secondary droplet atomization, leading to formation of an aerosol cloud of polydisperse child droplets appears to be promising. It is topical to assess the influence of properties of liquid and gas medium on the position of transition boundaries between the regimes of drop collisions and characteristics of the formed child droplets. This article presents the experimental results for the characteristics of drop collisions at various temperatures of the liquid and gas-vapor mixture and water vapor concentration in the latter with the aim of developing the prospective heat and mass transfer gas-vapor technologies. For this purpose, we have created the experimental set-up that allows varying the relative humidity of gas-vapor mixture in the area of drop collisions from 20-100%, its temperature from 20-100 °C and the temperature of the liquid from 20-90 °C. The test fluid is water. The collisions are recorded by a high speed video camera. The consequences of collision and the boundaries between them on the regime maps are determined in accordance using the approach, distinguishing: bounce, coalescence, separation, and disruption.

Key words: *drop collision, regime, child droplets, vapor concentration, high temperature heating, gas-vapor mixture*

Introduction

An active interest, shown in the last 5-7 years in the studies of integral characteristics of the interaction of colliding liquid drops in a gas medium, is conditioned by the main objective, namely to identify the key mechanisms and to search for the regimes of controlling these processes in many modern promising technologies, e.g., fuel combustion in IC engines [1-3], fire-fighting [4], pharmaceuticals production [5], application of aerosol systems to determine the level of air pollution [6], etc. The objects of such studies include both homogeneous and two, three and multi-component drops of solutions, slurries, and emulsions. They can interact intensively in homogeneous, e.g., air, as well as in two- and multi-phase flows, in particular, gas-vapor or more complex mixtures based on combustion products of organic substances. As a consequence, the integral parameters of drop collisions depend on both the properties of the liquid (surface tension, viscosity, and density) and the gas medium. In this case, the properties of the latter, as a rule, change more significantly at temperature and humidity variation if compared to the liquid. Taking into account these factors, it becomes possible to control the characteristics of the so-called secondary atomization of liquid drops in collisions not only by varying the angles of attack, size ratios and the resulting velocity of the drops, but also the parameters of

* Corresponding author, e-mail: pavelspa@tpu.ru

the gas medium. Fuel and chemical engineering technologies are characterized by particularly great potential due to the usage of liquids and gas media with properties that vary over a wide range. In this regard, very essential are the known results of researches [7-16] received in recent years by the world scientific community in experiments and mathematical modelling.

The results of mathematical modelling of drop collisions in diesel aerosols were presented in [7]. The results of the study served to build spatial maps of regimes, taking into account Weber numbers, the ratio of sizes of initial drops, Δ , and dimensionless linear parameter of interaction, B . From their analysis it was established that drops of unequal size are most probably characterized by coalescence, *i.e.* their enlargement at motion in the combustion chamber. The experimental results of study [7] allowed formulating recommendations to change the characteristics (drop sizes, jet intersection angles, number of spray nozzles, *etc.*) of primary fuel atomization with the view of minimizing the coalescence frequency and increasing the completeness of evaporation and burnout of fuel with minimum anthropogenic emissions. It was supposed that evaporation can significantly change the regimes and consequences of drop collisions in the gas medium. It is especially difficult to predict the effect of this factor for multicomponent drops due to significant differences in the rates of their heating and evaporation. Therefore, it is essential to study these features by the example of one-component drops.

Rabe *et al.* [8] presented the results of binary collisions of water drops from 220 to 450 μm in size, moving with velocities of 3-10 m/s. The ratio of drop diameters was 0.5-1. The values of the Weber number were from 20-280. The following regimes of drop collisions were distinguished: stretching separation, coalescence and reflexive separation. For higher Weber numbers (120-280), coalescence was not detected. Only stretching and reflexive separations were observed. The collision regime maps were constructed to predict the formation of the so-called triple point, in the vicinity of which the stretching separation, coalescence and reflexive separation can occur. From the comparative analysis of the results of [7, 8] it should be noted that in considering the fuel drops, the position of this triple point depends not only on the Weber number or the dimensionless interaction parameter. The determinant and different-scale (relative to each other) role is played by the properties of the liquid: density, viscosity and surface tension.

In Finetello *et al.* [9], the influence of fluid viscosity on the characteristics of drop collisions was studied. Sucrose solutions with different concentrations (40% and 60%) were chosen as the test liquids. The collision regime maps for capillarity numbers of 0.1-1 were constructed. Experimental results [9] demonstrated that the higher the liquid viscosity is, the stronger the elasticity and internal friction forces are manifested. As a result, the regimes of bounce, coalescence and separation begin to dominate. At disruption, rather large fragments of liquid are formed, *i.e.* it is difficult to ensure the formation of a fine-dispersed cloud due to collisions of the initial drops. Only at extremely high values of the resulting velocities of the drop-projectile and the drop-target can their secondary atomization be enhanced.

Kollar *et al.* [10], the results of mathematical modelling of collision of liquid drops in a wind tunnel were presented. Such collision regimes as bounce, coalescence and disruption into secondary droplets (disintegration) were explored. Maps of drop collision regimes were described using Weber and Reynolds numbers, interaction parameters, and the ratio of drop sizes. The size distributions of liquid fragments in the laminar flow were calculated. It was shown that at the increase in velocity of the drops in the gas medium before their collision, they transit into a state of instability, *i.e.* they are significantly deformed relative to the spherical shape. As a consequence, the conditions conducive to their breakup and formation of a fine-dispersed liquid cloud are provided. Kollar *et al.* [10] is considered extremely important. The results presented in it served as a starting point for the development of the scientific direction, which consists

in controlling the size and number of secondary droplets formed during collisions of the initial ones. They are often called *child droplets* or *satellite droplets*. The terms *child droplets* or *satellite droplets* differ in that the *child droplets* include all formed secondary droplets, and the *satellite droplets* reckon in only the liquid fragments, formed during the disintegration of the bridge between colliding drops. It is worth noting the experimental and theoretical studies of child and satellite droplets, *e.g.*, [11-16].

Brenn *et al.* [11] considered drop collisions that lead to the formation of a polydisperse aggregate of satellite droplets. It was found out that a satellite droplet is formed when the Weber numbers are less than 49 and the linear interaction parameter is 0.57. Three satellite droplets was formed at a Weber number of 132 and a dimensionless interaction parameter equal to 0.44. The dependences of the probability (frequency) of formation of a certain number of satellite droplets on the critical Weber numbers were also determined in [11]. Pischke in [12], a large number of child droplets are formed from the initial drop in the so-called spontaneous disruption and stripping breakup. As a result of spontaneous disruption, the drop breaks up immediately. The spontaneous breakup occurs if the original drops are in a vibrational transformation mode (the shape is significantly different from the spherical one), *i.e.* within the Weber numbers from 12-80. Unlike the spontaneous breakup, the stripping breakup occurs at Weber numbers of 80-800 and is accompanied by the emergence of a large aggregate of child droplets [12]. Drop fragmentation and formation of satellite droplets were also studied in [13]. The number of satellite droplets and their sizes (in comparison with similar parameters of the initial drops) were shown to depend mainly on the viscosity of the liquid. The latter can vary significantly due to the introduction of drops of specialized additives and impurities.

Articles [14-16] examined the collisions of the drops of complex composition. The emergence of satellite droplets during the stretching separation for binary collisions of propanol, water-sugar solution and acetone drops were investigated in [14]. Experimental studies and modelling for equal-sized drops were carried out. The effect of the size of colliding fragments and the viscosity of liquids on the characteristics of the satellite droplets formation is reviewed. A large number of satellite droplets is formed at a Weber number over 80 and an increase in their number with the growth of the interaction parameter B [14]. Sommerfeld *et al.* [15] presented the interaction regime maps for FVA1 oil and considered the effect of viscosity on the characteristics of drop collision due to the changes (from 23-100 °C) in the temperature of the oil. The mathematical modelling of collision of evaporating and burning n-decane drops was performed in [16]. It was established that evaporation decreases surface tension. When modelling collisions of igniting drops, the latter accelerate when approaching each other [16]. Assumptions were formulated to explain these features, the main of which implies that the drops significantly decrease in size during evaporation, and due to the gas-phase reaction, the pressure of gases around the drops increases. This increases the relative velocity of the drops and the frequency of their collisions. The effects of turbulent pulsations in the chemical reaction zone are not the least of the factors. The analysis of the results in [14-16] allows formulating a conclusion about a rather long list of factors, effects and processes that can affect the conditions and characteristics of collisions of multicomponent drops in a heated gas medium. For their detailed study, it is rational to conduct experiments according to the classical one-factor plan with the collision of one-component liquid drops in a gas medium with variable temperature and concentration of vapors.

The aim of this work is to experimentally study the regimes (bounce, separation, coalescence, disruption) and consequences (number and size of child droplets) of water drop collisions under intense heating and high concentration of water vapors. The scientific novelty

is that the limits for the transition from one collision mode to another have been first-time established at different heating temperatures of drops. Moreover, the differences in the characteristics of secondary droplets emerged when the initial drops collide have been shown. The sizes and quantity of child droplets are defined. The interaction regime maps for water are constructed taking into account its temperature and properties of the gas medium.

Experimental set-ups and methods

Figure 1 depicts the photo of the experimental set-up. When creating the set-up, it was necessary to take into account the features of high speed video recording of drop collisions in a gas-vapor mixture with a variable temperature and concentration of water vapors. Accordingly, specialized materials were required to manufacture the heating chamber. Heat-resistant quartz glass with a wall thickness of about 0.5 mm was used. The temperature of the gas medium in the heating chamber reached 100 °C. At higher temperatures, moisture condensation on the walls of the chamber worsened the conditions of video recording. Heating of the gas medium in the chamber was provided by an air blower with an electric heating element (power of 3400 W, air-flow of up to 800 Lpm, and operating temperature of up to 600 °C), increasing temperature in the area of drop collisions up to 100 °C for three minutes of operation. The pump with a flow rate of 0.2-3.6 Lpm immersed in the tank allowed varying the liquid-flow velocity at the outlet of the copper capillary. To ensure the liquid temperature of about 90 °C, the capillary was heated with a gas burner (fuel flow rate of 80 g per hour, power of 1.09 kW, and maximum temperature of 1300 °C) for one minute. When conducting a series of experiments in vapor medium, the air blower was replaced by a steam generator (constant steam supply of 120 g per minute). Two thermocouples (chromel-alumel, measuring range from -50 °C to 1200 °C, junction diameter of about 0.5 mm, error of ±1 °C, and thermal inertia time of about 1 second) were installed in the heating chamber to record temperatures of air and water drops. The experiments have revealed that the drops in the area of collisions cooled down by 4-8 °C relative to their temperatures at the outlet of the capillary. Therefore, the necessary and permissible conditions for the supply of drops have been empirically selected to take into account this feature and ensure the liquid temperature of about 90 °C in the zone of collisions.

Dosing and supply of drops were carried out using the ring element with installed capillaries of liquid supply. This allowed varying the angle of attack ($0 < \alpha_d < 90^\circ$) and the radius of drops (R_{d1}, R_{d2} in the range from 0.1-0.5 mm). By changing the voltage applied to the immersion pump, the values of velocity of the two generated drops varied (U_{d1}, U_{d2} in the range from 0.2-4 m/s). The high speed video camera with a resolution of 1152×864 and a frame rate from 3000-100000 fps was used to videotape the collision.

The videos were processed using the FASTCAM software. To define a collision mode, from 100-300 collisions of the drops were treated. The size and velocity of the drops, the angle of the attack, the distance between the centers of the drops when they collide, and the collision regimes were determined. The systematic error in measuring the size and velocity of drops as well as the angle of attack was 2.1%, 3.4%, and 1.8%, respectively. The random error in determining the size of the drops is 2.1%, their velocity – 3.4%, and the angle of attack – 3.1%. The size of the drops R_d was analyzed based on five measurements to determine the mean radius and to minimize the random error. The next step was to determine the standard deviation:

$${}^nS = [\sum_{i=1}^n (R_{av} - R_i)^2]^{0.5} / (n - 1)$$

where R_{av} is the mean radius of the drop and n is the number of measurements. Then, to detect gross errors the three-sigma rule was used. The standard deviation for the set of measurements

was calculated by ${}^nS_x = {}^nS/n^{0.5}$. The confidence interval (*i.e.* the absolute error of the set of measurements) was given by $\Delta R_d = {}^nS_x \cdot t(\alpha, n)$, where $t(\alpha, n)$ is the Student's coefficient. Errors in measuring the size of the drops, the angles of attack and the distance that passes the drop over a certain time were calculated similarly. These errors were conditioned by surface transformations of the drops during their motion in a gas environment and an insignificant change in their angle of attack due to the instability in operation of the immersion pump. The error in determining the velocity of the drops depended on the error of the set of indirect measurements. In this case, the velocity was a function of one variable $U = f(L)$. Since only the distance changed, while the time remained the same for all the experiments and was $t = n$ per fps, where n is the number of frames and fps is the frame frequency, then the error could be determined as $\Delta U = \Delta L/t$. The relative error of the set of indirect measurements was calculated by $\delta U = \Delta U/U_{av}$, where U_{av} is the mean velocity of the drop.

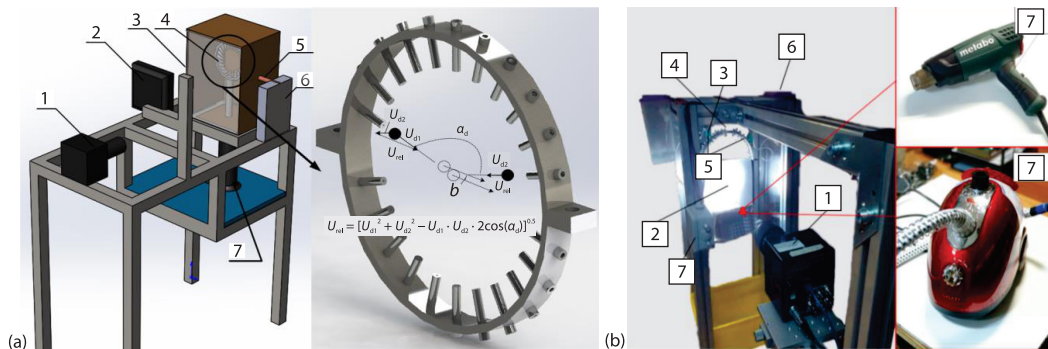


Figure 1. Schematic (a) and photo (b) of experimental set-up: 1 – high speed video camera, 2 – lighting system, 3 – heating chamber; 4 – ring carrier of capillaries of liquid supply, 5 – capillaries channel for liquid supply, 6 – tank with liquid and submersible pump, and 7 – supercharger of heated air or steam generator

Four regimes have been distinguished: bounce, coalescence, disruption, and separation. At a bounce there is an elastic collision of drops, and further they disperse without formation of new fragments and without destroying a superficial cover of each other. Coalescence characterizes the conditions, under which the drops coalesce into one and do not disintegrate with further movement. Separation is marked by the violation of the drops integrity without the formation of new fragments of liquid. Disruption differs from separation by the forming of secondary fragments as a result of disintegration, *i.e.* a group of satellite droplets is formed.

To calculate the number of fragments formed, the radius, r_{di} , of all visible (*i.e.* in the video recording area) child droplets and their number, N_{ti} , were measured. The volume of two drops before interaction, $V_0 = 4\pi(R_{d1}^3 + R_{d2}^3)/3$, and formed child droplets, $V_1 = 4\pi\sum r_{di}^3/3$, were calculated. Further, the number of the formed fragments, N_{ty} , was proportionally increased to ensure equality of fluid volumes before and after the collision. Thus, it was possible to take into account the liquid fragments outside the registration area. The next step in processing the experimental data involved calculating the ratio, S_1/S_0 , *i.e.* the surface area of child droplets, $S_1 = 4\pi\sum r_{di}^2$, to the initial surface area of the initial drops prior to interaction, $S_0 = 4\pi(R_{d1}^2 + R_{d2}^2)$.

A dimensionless linear interaction parameter $B = b/(R_{d1} + R_{d2})$ was used to control the centricity of the collision. Figure 2 demonstrates a scheme for determining the dimensionless interaction parameter. The dimensionless Weber number ($We = 2\rho R_{d1} U_{rel}^2/\sigma$) allows taking into account the drop size, velocity and surface tension simultaneously. The research results were generalized in the calculation of Weber number. The properties of water were

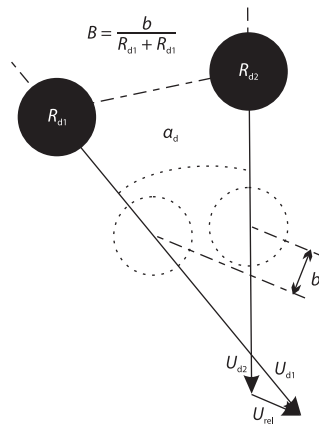


Figure 2. Scheme for determining the parameters during drop collision

taken in [17, 18]: at a temperature of 20 °C $\rho = 998 \text{ kg/m}^3$, $\sigma = 0.07269 \text{ N/m}$, $\mu = 0.0014 \text{ Pa}\cdot\text{s}$ and 90 °C $\rho = 958 \text{ kg/m}^3$, $\sigma = 0.0613 \text{ N/m}$, $\mu = 0.000237 \text{ Pa}\cdot\text{s}$.

To account for the specific conditions of drop collisions in promising gas-vapor-liquid systems, rather wide ranges of key parameters were chosen. In particular, the initial radius of the generated drops ranged from 0.2-1 mm, and their initial velocity was 0.2-4 m/s. The angle of attack was 0-90 °. The studies were carried out at two temperatures of water (20 °C and 90 °C) and gases in the chamber (20 °C and 100 °C). The concentration of water vapor in the gas-vapor mixture in the heating chamber varied from 20-100 % (a hygrometer with a measurement error of not more than 2% was used for monitoring). The Weber number varied within 0-220.

Figure 3 shows the images of colliding drops in the regimes of bounce and disruption. These illustrations reflect the effects of water and gas temperatures, as well as the concentration of water vapor in the gas on drop collisions and the formation of child droplets. In particular, in figs. 3(a) and 3(b) an increase in the temperature of the liquid and gas medium contributes to a significant fragmentation of the drops during collisions in the disruption mode due to a decrease in surface tension. Figures 3(c) and 3(d) demonstrates that the increase in the concentration of water vapor in the gas-vapor mixture intensifies the bounce of even quite large drops at their significantly higher relative velocities. This is mainly due to the increase in the pressure of the gas-vapor mixture and the repulsion of the approaching liquid fragments from each other.

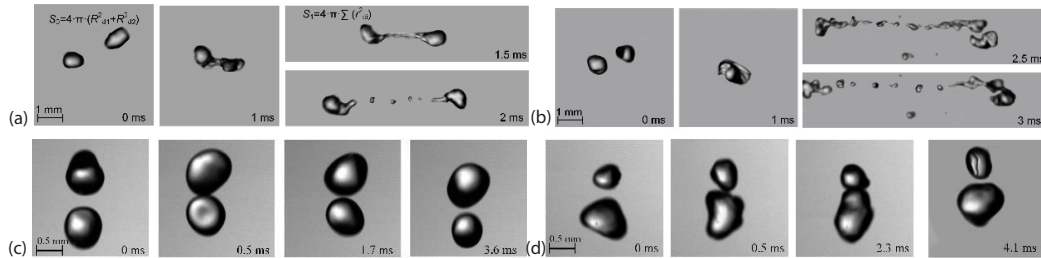


Figure 3. Effect of humidity and temperature of gas-vapor mixture and preliminary heating of water on the conditions of drop interaction; (a) $T_a \approx 20 \text{ }^\circ\text{C}$ and $T_d \approx 20 \text{ }^\circ\text{C}$, (b) $T_a \approx 100 \text{ }^\circ\text{C}$ and $T_d \approx 90 \text{ }^\circ\text{C}$, and (c) $T_d \approx 20 \text{ }^\circ\text{C}$ and $\gamma \approx 20\%$, and (d) $T_d \approx 20 \text{ }^\circ\text{C}$ and $\gamma \approx 100\%$

Results and discussion

Effect of water vapor concentration

The experiments have shown that the concentration of water vapor in the area of drop collisions has a significant impact on the collision regimes, the position of the transition boundaries between them and the calculated characteristics of child droplets. Collisions occurred at two relative concentrations of water vapor in the gas-vapor mixture, namely 20% and 100%. When the relative concentration of water vapor increases to 100%, the bounce area increases almost two times, fig. 4. This increase occurs both over the Weber number axis and over B -axis. Thus, at a high concentration of water vapor, the bounce is manifested at more centric

impacts of drops. Their coalescence requires a large kinetic energy in the collision region overcome the repulsive forces, caused by the vapor layer between the drops. The boundary between disruption and separation is shifted towards the large critical Weber numbers by 12% and 22%, respectively. This is also due to the vapor layer between the drops at the time of their approach, which leads to the deceleration of the drops just before their interaction begins. Consequently, there is an expansion of the coalescence zone with an increase in the concentration of water vapor in the gas medium.

Figure 5 shows the ratios of the free surface area of child droplets to the same parameter for drops before collision, as well as the size distribution of the formed fragments at $We \approx 150$. When increasing vapor concentration, disruption slows down, and to achieve this regime, the large Weber numbers are necessary. In this case, the increase of Weber number is possible both due to the growth of the size of the initial drops and the resulting velocity. The experiments have shown that the size of the initial drops have a significantly smaller effect on the characteristics of their disruption compared to the resulting velocity. This is mainly due to the fact that the kinetic energy in the collision zone is determined by the resulting velocity of the drops.

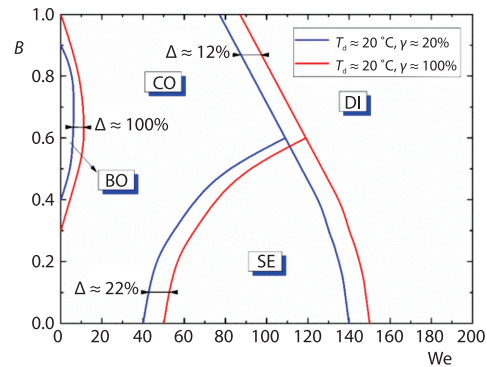


Figure 4. Effect of water vapor concentration in gas-vapor mixture on the boundaries between the regimes

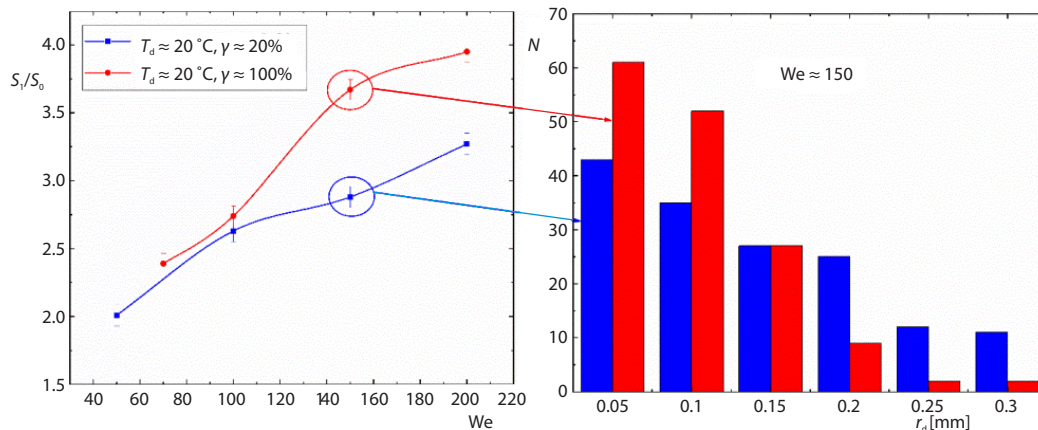


Figure 5. The S_1/S_0 vs. Weber number and the distribution of fragments over the radius at different γ

The observed differences in the distribution of child droplets with varying vapor concentrations in the collision region in fig. 5 are also associated with vapor layers between the drops. The latter can be formed whether by increasing the concentration of water vapor as a whole when using a steam generator or by the additional evaporation of the drops. The formation of such layers of increased density of the gas-vapor medium slows down the approach of drops, but only in a limited range of Weber number values. In particular, at $We > 70$, the colliding drops disintegrate despite the high pressure of the gas-vapor mixture. Thus, the forces of inertia become dominant. The comparative analysis has shown that the number of child droplets with a minimum recorded radius, $r_d \approx 0.05$ mm, increases by almost 40% during collisions

in a highly concentrated vapor medium, and the number of large fragments with $r_d > 0.2$ mm decreases. This may be linked to the fact that when the concentration of water vapor grows, the density and viscosity of the gas-vapor medium increase. As a consequence, viscous friction forces grow. In such conditions, at the same velocities and sizes of drops, the aerodynamic forces acting on them differ from the conditions of motion in the air. In addition, an important role is played by a significant reduction in the frequency of coalescence of secondary droplets, *i.e.*, the moving child droplets in the form of a large aggregate do not coalesce with each other, but intensely bounce. Therefore, the enlargement of child droplets due to secondary coalescence peculiar to motion in the air has not taken place.

Effect of liquid and gas medium temperatures

The experimental set-up allowed supplying liquid to the capillary tip with a temperature of up to 90 °C and then to the heating chamber, the temperature in which reached 100 °C. Thus, it became possible to consider three schemes, in which the drops and the gas medium in the collision region were heated alternately or jointly, figs. 6 and 7. As the temperature of the liquid increases, its surface tension decreases, which, in turn, leads to a decrease in the critical Weber numbers for the boundaries of the transitions between bounce, separation, and disruption, fig. 6. The bounce zone decreases ($\Delta \approx 57\%$) due to the weakening of the surface tension forces, *i.e.* the latter are not enough for elastic interactions of drops with each other. The boundaries of coalescence-to-disruption/separation transitions have been shifted by 27% and 45%, respectively. In addition, the area of separation has increased towards a larger dimensionless parameter B . Thus, the secondary atomization of drops enhances with an increase in their temperature.

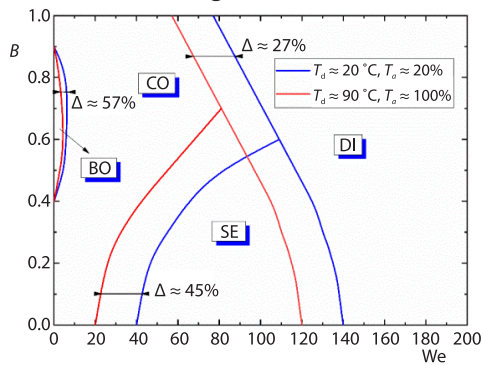


Figure 6. Effect of temperature on the boundaries of transitions between collision regimes

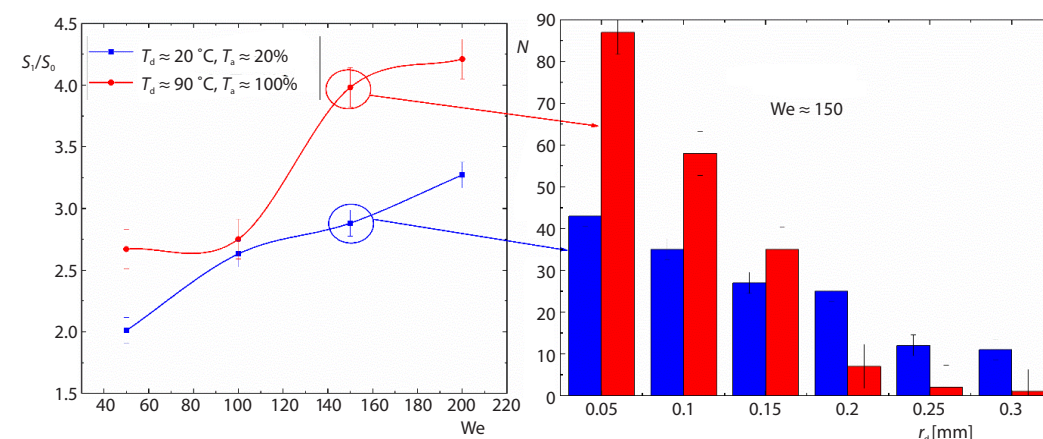


Figure 7. The S_1/S_0 vs. Weber number and distribution of fragments over the radius at different temperatures

Figure 7 demonstrates that when the air in the chamber and the liquid are heated, S_1/S_0 increases. This results in an increase in the number (almost by 50%) of child droplets

with a radius of less than 0.15 mm. In general, the increase in the number of formed fragments is explained by the change in the properties of the liquid during heating, *i.e.* by a decrease in viscosity and surface tension. Since the values of these properties of the liquid are reduced, the drop becomes unstable [19] and disintegrates. Due to the decrease in viscosity, the radius of the formed droplets decreases, since long transitions (deformation cycles) to spherical forms are specific for low viscosity liquids [19]. This promotes the fact that at low surface tension child droplets continue to break up after the collision of the initial drops due to rotating forces. The video recording has shown the formation of the polydisperse zones of secondary atomization of colliding drops.

When summarizing the results, the found trends are assumed to be enhanced in high temperature (over 500 °C) gas-vapor-liquid technologies. In particular, the significant disruption of drops is caused not only by their collisions, but also by swirling in turbulent flows, as well as by evaporation. The reduction of the size (due to evaporation) of both colliding drops and formed child droplets did not affect significantly the displacement of the boundaries between the regimes and the distribution of $N(r_d)$. This is due to the short time spent by drops in the video recording area. However, based on the analysis of the obtained videograms, it can be concluded that in real technologies, due to the high concentration of drops in the aerosol flows, the rates of their heating and evaporation will differ in different zones of the heating chambers. Hence, the values of S_1/S_0 will slightly deviate from those given in this study. In particular, the higher the concentration of drops in the aerosol is, the weaker the heating and evaporation are, and accordingly, the more intense the coalescence is. In the opposite case, the disruption of the heated liquid fragments enhances.

Conclusions

- The experiments have shown that an increase in the concentration of water vapor in the area of drop collisions shifts the transition boundary for disruption over the critical Weber number by 12% and increases the ratio of liquid surface areas by 35% (at $We \approx 150$). The obtained results are due to an increase in the pressure of the gas-vapor mixture around the drops and the intensification of their secondary atomization during collisions.
- When the temperature of the gas medium and liquid increases from 20 °C to 90-100 °C, there is a significant growth in the number of fragments formed (by 70%). Moreover, the boundary of the transition disruption is shifted by 27% towards the lower critical Weber number. This is caused by a significant decrease in viscosity and surface tension of the liquid.
- The results are of high practical importance for the development of secondary droplet atomization technologies in high temperature media and gas-vapor-liquid systems, as they illustrate the maps of initial drop collision regimes and the distributions of child droplets. The general conclusion is that in high temperature media the probability of separation of colliding drops is small. Based on the position of the triple point on the collision regime maps, it is possible to predict the minimum necessary conditions for intensive secondary atomization. Since most of modern models use empirical constants and expressions for the mean size of child droplets when studying drop collisions, the presented distributions can be applied to approximate the results of mathematical modelling to experimental data by considering the effects of water vapor concentrations, as well as the temperatures of the liquid and gas medium.

Acknowledgment

Research was funded by the Russian Science Foundation (project 18-71-/-10002).

Nomenclature

B	– dimensionless linear droplet interaction parameter	We	– Weber number
b	– distance between droplets' centers of mass, [m]	<i>Greek symbols</i>	
N	– number of child droplets	α_d	– angle of attack [°]
N_{vi}	– number of visible formed fragments	γ	– relative concentrations of water vapors in gas-vapor mixture, [%]
N_{vy}	– number of formed fragments	μ	– dynamic viscosity, [Pa·s]
R_{d1}	– radii of the first drop, [m]	Δ	– established deviations of the transition boundaries between collision regimes in the maps of parameters of collisions [%]
R_{d2}	– radii of the second drop, [m]	ρ	– density, [kgm ⁻³]
r_d	– radius of a child droplet [m]	σ	– surface tension, [Nm ⁻¹]
S_0	– total area of the initial drops, [m ²]	<i>Abbreviation</i>	
S_1	– total area of child droplets, [m ²]	BO	– bounce
T_a	– gas-vapor mixture temperature, [°C]	CO	– coalescence
T_d	– drop temperature, [°C]	DI	– disruption
U_{d1}	– velocity of the first drop, [ms ⁻¹]	SE	– separation
U_{d2}	– velocity of the second drop, [ms ⁻¹]		
U_{rel}	– resulting velocity of the drops, [ms ⁻¹]		
V_0	– total volume of drops before collision [m ³]		
V_1	– total volume of formed child droplets [m ³]		

References

- [1] Ganji, P., et al., Computational Optimization of Biodiesel Combustion Using Response Surface Methodology, *Thermal Science*, 21 (2017), 1B, pp. 465-473
- [2] Zhang, Z., et al., A Simulated Study on the Performance of Diesel Engine with Ethanol-Diesel Blend Fuel, *Thermal Science*, 17 (2013), 1, pp. 205-216
- [3] Jafarmadar, S., et al., Numerical Studies of Spray Breakup in a Gasoline Direct Injection Engine, *Thermal Science*, 15 (2011), 4, pp. 1111-1122
- [4] Vouros, A., et al., Experimental Study of a Water-Mist Jet Issuing Normal to a Heated Flat Plate, *Thermal Science*, 20 (2016), 2, pp. 473-482
- [5] Guildenbecher, D., et al., Secondary Atomization, *Experiments in Fluids*, 46 (2013), 3, pp. 371-402
- [6] Cao, F., et al., Numerical Modelling of Fine Particle Fractal Aggregates in Turbulent Flow, *Thermal Science*, 19 (2015), 4, pp. 1189-1193
- [7] Post, S., et al., Modelling the Outcome of Drop-Drop Collisions in Diesel Sprays, *International Journal of Multi-phase Flow*, 28 (2002), 6, pp. 997-1019
- [8] Rabe, C., et al., Experimental Investigation of Water Droplet Binary Collisions and Description of Outcomes with a Symmetric Weber Number, *Physics of Fluids*, 22 (2010), 4, 47101
- [9] Finotello, G., et al., Effect of Viscosity on Droplet-Droplet Collisional Interaction, *Physics of Fluids*, 29 (2017), 6, 67102
- [10] Kollar, L., et al., Modelling Droplet Collision and Coalescence in an Icing Wind Tunnel and the Influence of These Processes on Droplet Size Distribution, *International Journal of Multi-Phase Flow*, 31 (2005), 1, pp. 69-92
- [11] Brenn, G., et al., The Formation of Satellite Droplets by Unstable Binary Drop Collisions, *Physics of Fluids*, 13 (2001), 9, pp. 2463-2477
- [12] Pischke, P., Modelling of Collisional Transport Processes in Spray Dynamics, Ph. D. thesis, Aachen University, Aachen, Germany, 2014
- [13] Tjahjadi, M., et al., Satellite and Subsatellite Formation in Capillary Breakup, *Journal of Fluid Mechanics*, 243 (1992), Apr., pp. 297-317
- [14] Brenn, G., et al., Satellite Droplet Formation by Unstable Binary Drop Collisions, *Physics of Fluids*, 18 (2006), 8, 87101
- [15] Sommerfeld, M., et al., Modelling Droplet Collision Outcomes for Different Substances and Viscosities, *Experiments in Fluids*, 57 (2016), 12, 187
- [16] Ashna, M., et al., The LMB Simulation of Head-on Collision of Evaporating and Burning Droplets in Coalescence Regime, *International Journal of Heat and Mass Transfer*, 109 (2017), June, pp. 520-536
- [17] Finotello G., et al., Experimental Investigation of Non-Newtonian Droplet Collisions: the Role of Extensional Viscosity, *Experiments in Fluids*, 59 (2018), 7, pp. 59-113

- [18] Vargaftik, N., *et al.*, International Tables of the Surface Tension of Water/Journal of Physical and Chemical Reference Data, *12* (1983), 3, pp. 817-820
- [19] Volkov, R., *et al.*, Water Droplet Deformation in Gas Stream: Impact of Temperature Difference between Liquid and Gas, *International Journal of Heat and Mass Transfer*, *85* (2015), June, pp. 1-11